

Understanding large local CP violation in $B^\pm \rightarrow K^\pm \pi^+ \pi^-$ using dispersive methods

L. A. Heuser^{a,1,*} A. Reyes-Torrecilla^{a,2,†} C. Hanhart^{a,3}
 B. Kubis^{a,1} P. C. Magalhães^{a,4} T. Mannel^{a,5} and J. R. Peláez^{a,2,1}

¹*Helmholtz-Institut für Strahlen- und Kernphysik and Bethe Center for Theoretical Physics,
 Universität Bonn, 53115 Bonn, Germany*

²*Departamento de Física Teórica and IPARCOS, Universidad Complutense de Madrid, 28040 Madrid, Spain*

³*Institute for Advanced Simulation (IAS-4), Forschungszentrum Jülich, 52425 Jülich, Germany*

⁴*Departamento de Raios Cósmicos e Cronologia, Universidade Estadual de Campinas 13083-860, Campinas, Brazil*

⁵*Center of Particle Physics (CPPS), Theoretische Physik 1, Universität Siegen, 57068 Siegen, Germany*

We utilize the universality of pion-pion ($\pi\pi$) final-state interactions at small invariant masses to understand their enhanced local CP violation in $B^\pm \rightarrow K^\pm \pi^+ \pi^-$, using a dispersive approach. From a fit to the integrated CP-asymmetry data, we successfully predict the Dalitz-plot kinematic distribution of the asymmetry in the low-energy $\pi\pi$ region, including the large local CP violation recently observed by LHCb. An essential role is played by the contributions of isospin 2. This formalism, whose parameters have a physical meaning, can be adapted straightforwardly to other systems with CP violation enhanced by final-state interactions.

Introduction—Non-leptonic decays of heavy mesons are notoriously difficult to describe theoretically. Although QCD factorization (QCDF) methods exist for two-body decays, three-body decays remain a theoretical challenge [1]. In the Standard Model, CP violation (CPV) is induced by an interplay of the weak phase from the Cabibbo–Kobayashi–Maskawa (CKM) matrix [2, 3] and the strong phases of hadronic matrix elements. In three-body decays, strong phases depend on two kinematic variables, resulting in a complex structure in the Dalitz-plot distribution of CP asymmetries. This has been confirmed by LHCb [4–6] for $B^\pm \rightarrow h_1^\pm h_2^+ h_2^-$ decays, where $h_n^\pm = \pi^\pm, K^\pm$.

While integrated CP asymmetries are only a few percent, LHCb observed, and reaffirmed in their recent 5.9 fb^{-1} integrated luminosity analysis [7], one order of magnitude larger asymmetries in localized Dalitz-plot regions. Through amplitude analyses with simple resonance models [8–10], LHCb has attributed these large localized asymmetries to hadronic final-state interactions (FSI), particularly in the S wave. For instance, they claim that the $\pi\pi \rightarrow K\bar{K}$ S -wave rescattering contribution to $B^\pm \rightarrow \pi^\pm K^+ K^-$ has “the largest CP asymmetry reported to date for a single amplitude of $(-66 \pm 4 \pm 2\%)$ ” [10]. The dominant role of S -wave $\pi\pi \leftrightarrow K\bar{K}$ also naturally explains [11–14] the opposite integrated CP asymmetries in $B^\pm \rightarrow \pi^\pm \pi^+ \pi^-$ and $B^\pm \rightarrow \pi^\pm K^+ K^-$ in the 1 to 1.5 GeV invariant-mass region of the pair $h_2^+ h_2^-$.

The rich CPV Dalitz-plot structure of B -meson decays cannot be reproduced by a leading-order calculation in QCDF, even in terms of pseudo-two-particle processes [15]. However, a correct implementation of the

strong phases is crucial in any CPV analysis. Thus, an approach that treats the hadronic part of the decay systematically is of utmost importance. In this letter, we bring forth an important step in this direction.

To illustrate the method in its simplest form, we focus on $B^\pm \rightarrow K^\pm \pi^+ \pi^-$, as the kaon spares us from symmetrization complications and because the observed large local CPV lies at the $m_{\pi\pi} \leq 1.5\text{ GeV}$ invariant-mass region (cf. Fig. 3 in Ref. [7]), which is particularly intriguing. In existing $B^\pm \rightarrow h_1^\pm h_2^+ h_2^-$ amplitude analyses [9, 10], resonances are commonly included as Breit–Wigner (BW) parametrizations or variants thereof within isobar formalisms; however, this approach is in general model- and channel-dependent, and if there is more than one resonance in a partial wave or complex couplings are used, it violates unitarity. In addition, it does not allow for a proper inclusion of chiral symmetry constraints, nor a description of the isoscalar scalar $\pi\pi$ scattering data and the non-BW-like $f_0(500)$ and $f_0(980)$ resonances that appear therein [16]. Moreover, non-resonant partial waves are usually ignored. By construction, our method is consistent with unitarity and incorporates the high-accuracy phase-shift information available for the two-pion system [17–21]. As a first step, we develop our method within the elastic $\pi\pi$ scattering region, in practice $m_{\pi\pi} < 2M_K \sim 1\text{ GeV}$, since it contains most of the large local CP asymmetry observed in $B^\pm \rightarrow K^\pm \pi^+ \pi^-$, which appears with both signs in this mass regime.

Apart from the universality of FSI, we make three assumptions:

1. The weak interaction produces hadrons on a small distance scale, forming a “source” for outgoing hadrons, constructed in the spirit of [22].

2. For small $m_{\pi\pi}$, the pion pair has a large recoil against the BK system, of the order of the B -meson mass, M_B . Hence, the $K\pi$ invariant mass is $\mathcal{O}(M_B)$, and the kaon final-state rescattering is negligible.

^a These authors contributed equally to this work.

* heuser@hiskp.uni-bonn.de

† albre01@ucm.es

3. Left-hand cuts, e.g., from $B \rightarrow D^* \bar{D}_s$, followed by $D^* \rightarrow D\pi$, with the remaining $D\bar{D}_s$ system transitioning to πK , can be approximated as providing (CP-even) constant imaginary parts and, as such, subsumed in the source terms.

In such a picture, all relevant energy dependencies and singularities are driven by the FSI of the outgoing pion pair, of long-distance nature and thus universal.

Notation—The $B^\pm(p_B) \rightarrow K^\pm(p_K)\pi^+(p_+)\pi^-(p_-)$ decay is characterized by the $s = (p_+ + p_-)^2 \equiv m_{\pi\pi}^2$ and $t = (p_K + p_+)^2 = (p_B - p_-)^2 \equiv m_{K\pi}^2$ Mandelstam variables. In the following, we work with partial-wave amplitudes of given angular momentum and isospin I . For $m_{\pi\pi} < 1$ GeV, those of relevance are the isoscalar $S0$ wave, featuring the $f_0(500)$ and $f_0(980)$ resonances, the isovector P wave with the prominent $\rho(770)$, and the isospin-2 $S2$ wave, free of resonances. We checked that D waves have a negligible effect in this range. Since the $f_0(980)$ lies almost at the $K\bar{K}$ threshold and couples strongly to two kaons, it is convenient to use a $\pi\pi$ - $K\bar{K}$ coupled-channel formalism, even in the elastic region, and split the $S0$ wave according to $\mathcal{A}_{S0}^\pm = \mathcal{A}_{S0n}^\pm + \mathcal{A}_{S0s}^\pm$, where the two parts are connected to the non-strange- and strange-quark operator structures of the source. The decay amplitude has the compact form

$$\mathcal{P}^\pm(s, t) = \sum_i f_i(s, t) \mathcal{A}_i^\pm(s) \quad (1)$$

with $i \in \{S0n, S0s, S2, P\}$. The dependence on the angle θ between the K^\pm and the π^\mp is carried by $f_i(s, t) = 1$ for $i = S0n, S0s, S2$ and $f_P(s, t) = t - u = g(s)z(s, t)$, where $z(s, t) = \cos\theta$. Here $g(s) = -\sigma_\pi(s)\lambda^{1/2}(s, M_K^2, M_B^2)$, $\sigma_h(s) = \sqrt{1 - 4M_h^2/s}$, and $\lambda(x, y, z) = x^2 + y^2 + z^2 - 2xy - 2yz - 2xz$.

Universal final-state interaction—The starting point for the dispersive analysis is the discontinuity relation for the production partial-wave amplitudes along the pion-pair cut at $s > 4M_\pi^2$. For $i = S2, P$ this reads

$$\text{Disc } \mathcal{A}_i^\pm(s) = 2i\rho_\pi(s)\mathcal{M}_i(s)^* \mathcal{A}_i^\pm(s), \quad (2)$$

where $\rho_h(s) = \sigma_h(s)/16\pi$. Note the appearance of the $\pi\pi$ scattering partial-wave amplitude $\mathcal{M}_i(s)$, which, being CP-invariant, carries no \pm superscript. For the elastic case, $\mathcal{M}_i(s) = e^{i\delta_i(s)} \sin \delta_i(s)/\rho_\pi(s)$, where δ_i is its phase shift. This leads to a closed-form solution [23]:

$$\mathcal{A}_i^\pm(s) = P_i(s)\Omega_i(s)\bar{\mathcal{A}}_i^\pm, \quad (3)$$

which describes the low-energy universal pion-pair interactions, contained in the Omnès function for the elastic case:

$$\Omega_i(s) = \exp \left\{ \frac{s}{\pi} \int_{4M_\pi^2}^{\infty} ds' \frac{\delta_i(s')}{s'(s' - s - i\epsilon)} \right\}, \quad \Omega_i(0) = 1. \quad (4)$$

The constants $\bar{\mathcal{A}}_i^\pm$ parametrize the source, and $P_i(s)$,

with $P_i(0) = 1$, is a function free of right-hand cuts up to inelastic thresholds, to be parametrized by a polynomial. This form automatically satisfies Watson's theorem [24] (cf. also Refs. [12, 25–27]), stating that in the elastic case, the phases of the production and scattering partial-wave amplitudes coincide. The $P_i(s)$ are often well approximated by 1 (cf. Ref. [28] for $B \rightarrow J/\psi\pi^+\pi^-$), or, at most, as linear polynomials, whose slopes are free parameters. While the Omnès function captures all the universal elastic hadron-hadron interactions, the $P_i(s)$ are reaction-specific and absorb the uncertainty in the high-energy extension of the phases and, to some extent, crossed-channel effects [29].

For the $S0$ wave, Eq. (2) in coupled channels just has one more term accounting for $K\bar{K} \rightarrow \pi\pi$ rescattering:

$$\begin{aligned} \text{Disc } \mathcal{A}_{S0n}^\pm &= 2i(\mathcal{M}_{11}\rho_\pi\mathcal{A}_{S0n}^\pm + \mathcal{M}_{12}^*\rho_K\mathcal{B}_{S0n}^\pm), \\ \text{Disc } \mathcal{A}_{S0s}^\pm &= 2i(\mathcal{M}_{11}\rho_\pi\mathcal{A}_{S0s}^\pm + \mathcal{M}_{12}^*\rho_K\mathcal{B}_{S0s}^\pm), \end{aligned} \quad (5)$$

where \mathcal{B}_i^\pm is the corresponding $K\bar{K}$ production amplitude and, for brevity, we have suppressed the s dependence. The $\mathcal{M}_{ij}(s)$ are the scalar scattering partial-wave amplitude elements between channels $1 = \pi\pi$ and $2 = K\bar{K}$. They are parametrized in terms of the $\pi\pi \rightarrow \pi\pi, K\bar{K}$ phase shifts together with the elasticity $\eta(s)$ [30–32].^b There are no closed-form solutions of Eq. (5) (and the corresponding discontinuities for $\mathcal{B}_{S0n}^\pm, \mathcal{B}_{S0s}^\pm$), but a matrix solution Ω_{ij} can be computed numerically from an integral equation, with the conditions $\Omega_{11}(0) = 1, \Omega_{12}(0) = 0$ [28, 34–41]. Here we use the results of Ref. [41]. The linear combinations corresponding to non-strange and strange sources are then given as

$$\Omega_{S0n} \equiv \Omega_{11} + \frac{1}{2}\Omega_{12}, \quad \Omega_{S0s} \equiv \Omega_{12}. \quad (6)$$

We allow for a common polynomial $P_{S0n}(s) \equiv P_{S0s}(s)$ multiplying the complete $S0$ wave. The complete $B^\pm \rightarrow K^\pm\pi^+\pi^-$ amplitude parametrization reads

$$\mathcal{A}^\pm(s, t) = \sum_i f_i(s, t) P_i(s) \Omega_i(s) \bar{\mathcal{A}}_i^\pm, \quad (7)$$

Source terms—Besides the polynomial slope parameters, the constants $\bar{\mathcal{A}}_i^\pm$ remain as free parameters. They specify the sources and their evaluation involves the two matrix elements $M_{u\bar{u}}$ and $M_{c\bar{c}}$, where $M_{q\bar{q}} = \langle K^+\pi^+\pi^- | (\bar{b}q)(\bar{q}s) | B^+ \rangle$ in the limit $m_{\pi\pi} \rightarrow 0$, plus the CP conjugates for the B^- decay. Here $(\bar{q}q')$ is the usual weak-interaction current, omitting Dirac structures for simplicity. The relevant effective weak Hamiltonian reads

$$H_{\text{eff}} = \frac{G_F}{\sqrt{2}} \left(|V_{cb}^* V_{cs}| (\bar{b}c)(\bar{c}s) + e^{i\gamma} |V_{ub}^* V_{us}| (\bar{b}u)(\bar{u}s) \right). \quad (8)$$

^b The coupled-channel $I = 0$ S -wave formalism has previously been applied in the context of CPV for D -meson two-body decays [33].

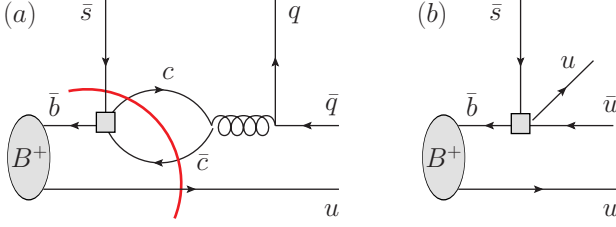


FIG. 1. Typical topologies for quark-level decays of $B^+ \rightarrow K^+ \pi^+ \pi^-$ (a) with and (b) without charm loop. The gray box represents the flavor-changing weak decay process, which contains the CKM elements and CPV phase. For $q = s$, the operator in diagram (a) provides a $\bar{s}s$ source, for $q = u$ or d a $\bar{u}u$ or $\bar{d}d$ source. The red line indicates the cut that generates an imaginary part. Diagram (b) provides a $\bar{u}u$ source.

In the standard parametrization [42] of the CKM matrix, V_{ub} carries the weak CPV phase γ , while V_{cb} , V_{cs} , and V_{us} are real. In terms of the Wolfenstein parametrization [43], $M_{u\bar{u}}$ is suppressed relative to $M_{c\bar{c}}$ by a factor $\lambda^2 \sim 0.04$. However, this suppression is partially compensated for by the loop needed to annihilate the $c\bar{c}$ pair, cf. Fig. 1(a), whereas the $u\bar{u}$ pair can be part of the light-meson pair in the final state, cf. Fig. 1(b). The $c\bar{c}$ loop hadronizes as charmed-meson loops, e.g., $\bar{D}^{(*)}D_s^{(*)}$; this mechanism generates CP-even phases (cf. Refs. [15, 44]), indicated by the $c\bar{c}$ cut (red line) in Fig. 1(a), beyond those coming from the Omnès functions. These phases are related to the charm-mass short-distance scale and will therefore lead to strongly varying effects near the charm thresholds. In the kinematic regions we consider, we do not expect strong energy dependence, and thus the phases can be subsumed in the $\bar{\mathcal{A}}_i^\pm$ sources. On the other hand, we assume the imaginary parts of the light-meson pair production from $M_{u\bar{u}}$ before FSI to be negligible, as similar quark-level loops are severely CKM-suppressed, and we neglect residual rescattering with the outgoing kaon. The latter could be tackled in the future with more complicated three-body dispersive equations [45–48]. As a result, we parametrize the source term as

$$\bar{\mathcal{A}}_i^\pm = \hat{A}_i + e^{\pm i\gamma} \hat{B}_i = a_i + ic_i \pm ib_i, \quad (9)$$

where the \hat{A}_i contain a CP-even constant imaginary part due to charm loops, while the \hat{B}_i are real. The parameters $a_i = \text{Re}\hat{A}_i + \hat{B}_i \cos \gamma$, $c_i = \text{Im}\hat{A}_i$, and $b_i = \hat{B}_i \sin \gamma$ will be determined by the fit.

Since our source parameters have a physical interpretation, their flavor structure allows us to reduce their number. First, \mathcal{A}_{S0s}^\pm refers to an isoscalar scalar pion pair emerging from an $\bar{s}s$ source through $K\bar{K} \rightarrow \pi\pi$ rescattering. However, the CPV phase γ is attached to $M_{u\bar{u}}$. Accordingly, we set the parameter b_{S0s} to zero. Moreover, the $c\bar{c}$ pair cannot produce a pion pair of isospin 2, and since in our approximation only those matrix elements have a CP-even imaginary part, c_{S2} has to vanish. Thus, there are three source parameters each for non-strange

isoscalar scalar and isovector vector partial waves, and two each for the strange isoscalar scalar and the isotensor scalar ones. Altogether, there are ten real parameters to parametrize the two CP-conjugated production vertices of four partial waves, plus three real slope parameters in the P_i polynomials.

The $\pi\pi$ P -wave spectrum can be significantly affected by ρ - ω interference in reactions that show strong production of the isoscalar $\omega(782)$. The smallness of the violation of isospin symmetry is compensated for by an enhancement of $\mathcal{O}(M_\omega/\Gamma_\omega) \approx 90$ through the narrow ω propagator. The strength of ρ - ω mixing can be gleaned directly from the electromagnetic pion form factor if the production strength of the ω relative to the ρ is known from the flavor structure of the source [28]. As illustrated in Fig. 1, diagram (b) provides a $\bar{u}u$ source, while diagram (a) generates either $\bar{u}u + \bar{d}d$ or $\bar{s}s$. However, since the $\bar{q}q$ pair from the hard gluon cannot be a colorless source for the pion pair, one of those quarks must combine into the charged kaon. This prevents the production of a $\bar{d}d$ pair from the gluon. The resulting pure $\bar{u}u$ source favors the ω by a factor of 3 compared to electromagnetic production. We incorporate it by multiplying Ω_P by $1 + 3\epsilon_{\rho\omega}s/(M_\omega^2 - s - iM_\omega\Gamma_\omega)$ with the known ρ - ω mixing strength $\epsilon_{\rho\omega}$ [49–51]. To simplify expressions below, we do not show the ω contribution individually, but understand it as part of the $\pi\pi$ P wave.

All in all, we arrive at the following expression for the $B^\pm \rightarrow K^\pm \pi^+ \pi^-$ differential decay count rates

$$\begin{aligned} \Gamma^\pm(s, z) &\equiv \frac{d^2\Gamma^\pm}{d\sqrt{s}dz}(s, z) = -g(s)\sqrt{s} \sum_{i,j} f_i f_j P_i P_j \\ &\times \left\{ \text{Re}(\Omega_i \Omega_j^*) (a_i a_j + b_i b_j + c_i c_j) + \text{Im}(\Omega_i \Omega_j^*) 2a_i c_j \right. \\ &\quad \left. \pm 2 \left[\text{Re}(\Omega_i \Omega_j^*) c_i b_j + \text{Im}(\Omega_i \Omega_j^*) a_i b_j \right] \right\}. \end{aligned} \quad (10)$$

Here, we focus on the difference due to CPV, which in the elastic regime leads to our main result:

$$\begin{aligned} \Delta\Gamma_{\text{CP}}(s, z) &\equiv \Gamma^-(s, z) - \Gamma^+(s, z) = 4g(s)\sqrt{s} \sum_{i,j} f_i f_j \\ &\times P_i P_j |\Omega_i| |\Omega_j| \left[a_i b_j \sin(\delta_i - \delta_j) + c_i b_j \cos(\delta_i - \delta_j) \right]. \end{aligned} \quad (11)$$

It is so simple because, in this regime, the production amplitude phase is just the $\pi\pi$ scattering phase shift δ_i . Moreover, the Ω_{S0n} and Ω_{S0s} phases are equal. The size of $\Delta\Gamma_{\text{CP}}(s, z)$ is determined by comparing to the sum of differential count rates, i.e., $\Sigma\Gamma(s, z) \equiv \Gamma^-(s, z) + \Gamma^+(s, z)$, obviously CP-even.

The presented formalism can be compared to earlier approaches; see, e.g., Refs. [52–55]. Most of these papers start from a factorization of the hadronic matrix elements into a heavy-to-light transition form factor and a light-meson form factor in the timelike region. The latter contains the universal soft rescattering also discussed

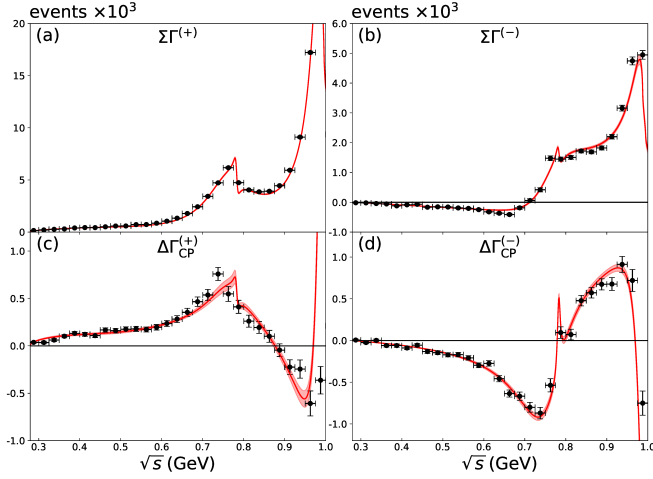


FIG. 2. Fit to the projected event distributions defined in Eq. (12), versus LHCb data [7] (supplemental material). We show (a) the angle-symmetric sum of yields, (b) the angle-asymmetric sum of yields, (c) the angle-symmetric CP-violating difference of yields, and (d) the angle-asymmetric CP-violating difference of yields.

above, which was previously either modeled or captured by an Omnès representation, however, omitting the non-resonant isospin-2 contribution. Within QCD factorization the Wilson coefficients contain imaginary parts from charm loops. To this end, a factorization approach can model our source terms, however, we employ a simple parametrization of the sources, which even has a clear physical interpretation.

Very recently, LHCb [7] (supplemental material) has provided high-statistics data with uncertainties on $\Gamma^\pm(s, z)$, integrated or “projected” separately over the forward ($z = \cos\theta > 0$) and backward ($z < 0$) regions, to be denoted by $>$ and $<$ superscripts, respectively. In our formalism, the nontrivial z -dependence appears linearly in the amplitude through $f_P(s, t)$. We can take advantage of these projections by defining

$$\begin{aligned}\Delta\Gamma_{\text{CP}}^{(\pm)}(s) &= \Delta\Gamma_{\text{CP}}^{>}(s) \pm \Delta\Gamma_{\text{CP}}^{<}(s), \\ \Sigma\Gamma^{(\pm)}(s) &= \Sigma\Gamma^{>}(s) \pm \Sigma\Gamma^{<}(s),\end{aligned}\quad (12)$$

to study differential decay rates not just in CP-symmetric and -antisymmetric combinations, but simultaneously in forward-backward symmetric or antisymmetric ones. The above definitions are useful for disentangling different partial-wave contributions. Hence, in Fig. 2 we show the data following these combinations.

Fit results—We average our results over the same 25 MeV-wide bins in which data were provided. Since the data are neither acceptance corrected nor background subtracted, we follow the method described by LHCb [7] to correct for the former. To correct for the latter, we add a linearly rising, non-interfering background to the data uncertainty.

The fit is shown in Fig. 2 as a red band. Its stability

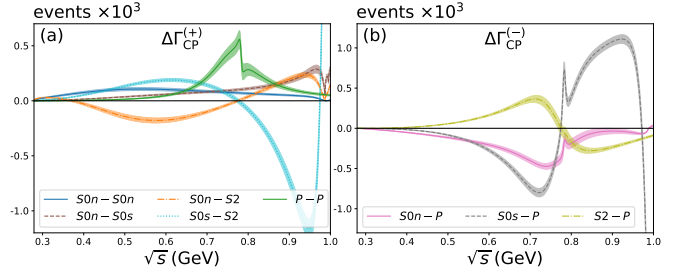


FIG. 3. The most relevant contributions to the projected $\Delta\Gamma_{\text{CP}}^{(\pm)}(s)$ distributions. Note the relevance of the $S2$ wave.

within uncertainties has been tested against a gradual increase of the relative error for all data points, simulating a systematic error, and against variations of the fit range below the two-kaon threshold. We checked that including an isoscalar tensor partial wave (restricted to not exceeding the data in the $f_2(1270)$ mass range), or CPV real parts in the source constants, does not significantly improve the data description. Moreover, we checked that releasing the constraints on the ω couplings to the source and $b_{S0s} = 0$ for \mathcal{A}_{S0s}^\pm returns values consistent with the constraints themselves. The error bands are generated using bootstrapping and imposing the confidence limits on the $\chi^2/\text{d.o.f.}$ as prescribed in Ref. [56].

Discussion—The relevance of different contributions to the two CPV distributions is illustrated in Fig. 3. The advantage of the approach presented here is that its parameters have a clear physical meaning. For example, the CP-even imaginary parts of the source terms, c_i , are due to $c\bar{c}$ -loops, related to open-charm meson pairs in hadronic terms. The presence of a ρ peak in $\Delta\Gamma_{\text{CP}}^{(+)}$, as seen in Figs. 2 and 3, illustrates the need for such a contribution, since according to Eq. (11) it scales as $c_P b_P |\Omega_P|^2$. Moreover, the isotensor S wave, \mathcal{A}_{S2}^\pm , is essential for the description of $\Delta\Gamma_{\text{CP}}^{(+)}$, interfering with the strange and non-strange isoscalar S waves. It is also required for an accurate description of $\Delta\Gamma_{\text{CP}}^{(-)}$, interfering with the ρ . The isotensor amplitude was not considered in earlier studies, since it does not contain any resonance.

Finally, we have only fitted projected CP-odd distributions. However, our primary goal is to describe the CPV asymmetry in $B^\pm \rightarrow K^\pm \pi^+ \pi^-$ observed by LHCb in localized regions of their Dalitz-plot analysis. This asymmetry reads

$$\mathcal{A}_{\text{CP}}(s, t) = \frac{\Delta\Gamma_{\text{CP}}(s, z(s, t))}{\Sigma\Gamma(s, z(s, t))} = \frac{\Gamma^-(s, t) - \Gamma^+(s, t)}{\Gamma^-(s, t) + \Gamma^+(s, t)}. \quad (13)$$

Since $\Gamma^\pm(s, t) \geq 0$, it follows that $|\mathcal{A}_{\text{CP}}(s, t)| \leq 1$. Given that our approach is limited to $s \leq 1 \text{ GeV}^2$, in Fig. 4 we only show the corresponding low- s section of the Dalitz plot. In Fig. 4(a), we reproduce the LHCb raw asymmetry, extracted from Fig. 3 in Ref. [7]. Note the use of an adaptive binning with a constant number of events per bin.

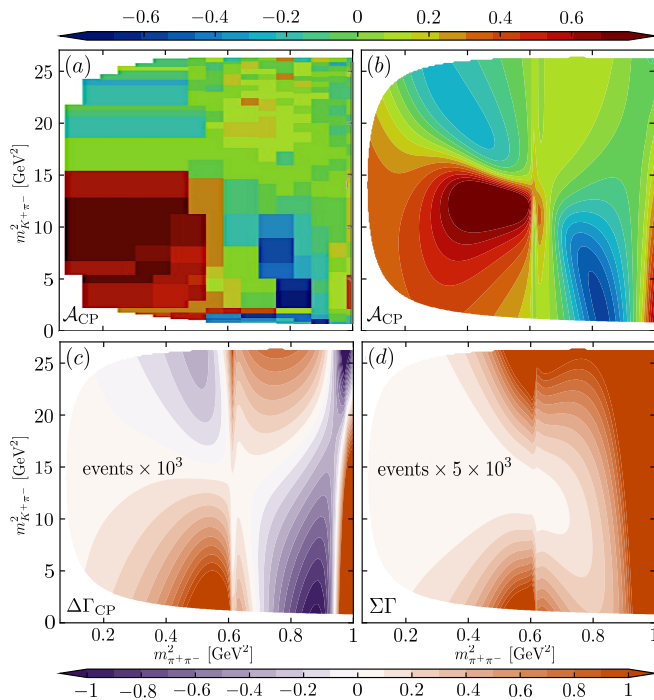


FIG. 4. $B^\pm \rightarrow K^\pm \pi^+ \pi^-$ CP asymmetry, distributed over the Dalitz plot section $m_{\pi^+\pi^-}^2 \leq 1 \text{ GeV}^2$. (a) LHCb binned raw asymmetry \mathcal{A}_{CP} , taken from Fig. 3 in Ref. [7]. (b) \mathcal{A}_{CP} from our analysis. (c) CP-violating difference $\Delta\Gamma_{CP}$. (d) CP-conserving sum $\Sigma\Gamma$.

With all parameters fixed, our model predicts the \mathcal{A}_{CP} Dalitz plot, which is shown in Fig. 4(b). The agreement between the data and our model is remarkable, considering that both the data and our results correspond to central values whose uncertainties cannot be shown in this plot. In particular, we reproduce the two localized regions with large local CPV, $|\mathcal{A}_{CP}(s, t)| \geq 60\%$, shown in dark red or blue. Since a small CP-even denominator

amplifies \mathcal{A}_{CP} , the predicted CP-violating numerator $\Delta\Gamma_{CP}$ is shown in Fig. 4(c) as well as the CP-even denominator in Fig. 4(d).

Summary and conclusions—We have presented a dispersive method to quantify the contribution of low-invariant-mass pion-pion rescattering to final-state interactions in $B^\pm \rightarrow K^\pm \pi^+ \pi^-$ and their CP-violating asymmetries. The advantage of our method is that it can incorporate high-precision universal $\pi\pi$ low-energy interactions. This also includes the commonly neglected non-resonant isospin-2 contribution, which is found to play an essential role. Once the parameters are fixed from the angular-integrated decay data from LHCb, we can predict the CP-asymmetry Dalitz-plot distribution, including the remarkable presence of large local CP asymmetries. Our approach illustrates the role of low-energy final-state interactions in enhancing CP violation in localized kinematic regions, and can be applied to other similar systems in the future.

Acknowledgments—This work was partially motivated during the preparations of the newly accepted Color meets Flavor cluster. Financial support by the MKW NRW under funding code NW21-024-A, by the Konrad-Adenauer-Stiftung e.V. with funds from the BMBF, the Spanish Grant PID2022-136510NB-C31 funded by MCIN/AEI/ 10.13039/501100011033, the European Union’s Horizon 2020 research and innovation program under grant agreement No. 824093 (STRONG2020), the Brazilian funding FAEPEX grant 2030-24, and INCT-FNA CnPq grant, is gratefully acknowledged. Th.M. was supported by the Deutsche Forschungsgemeinschaft (DFG, German Research Foundation) under grant 396021762 – TRR 257 “Particle Physics Phenomenology after the Higgs Discovery.” C.H. thanks the CAS President’s International Fellowship Initiative (PIFI) under Grant No. 2025PD0087 for partial support.

-
- [1] S. Kränkl, T. Mannel, and J. Virto, *Nucl. Phys. B* **899**, 247 (2015), arXiv:1505.04111 [hep-ph].
 - [2] N. Cabibbo, *Phys. Rev. Lett.* **10**, 531 (1963).
 - [3] M. Kobayashi and T. Maskawa, *Prog. Theor. Phys.* **49**, 652 (1973).
 - [4] R. Aaij *et al.* (LHCb), *Phys. Rev. Lett.* **111**, 101801 (2013), arXiv:1306.1246 [hep-ex].
 - [5] R. Aaij *et al.* (LHCb), *Phys. Rev. Lett.* **112**, 011801 (2014), arXiv:1310.4740 [hep-ex].
 - [6] R. Aaij *et al.* (LHCb), *Phys. Rev. D* **90**, 112004 (2014), arXiv:1408.5373 [hep-ex].
 - [7] R. Aaij *et al.* (LHCb), *Phys. Rev. D* **108**, 012008 (2023), arXiv:2206.07622 [hep-ex].
 - [8] R. Aaij *et al.* (LHCb), *Phys. Rev. Lett.* **124**, 031801 (2020), arXiv:1909.05211 [hep-ex].
 - [9] R. Aaij *et al.* (LHCb), *Phys. Rev. D* **101**, 012006 (2020), arXiv:1909.05212 [hep-ex].
 - [10] R. Aaij *et al.* (LHCb), *Phys. Rev. Lett.* **123**, 231802 (2019), arXiv:1905.09244 [hep-ex].
 - [11] B. Bhattacharya, M. Gronau, and J. L. Rosner, *Phys. Lett. B* **726**, 337 (2013), arXiv:1306.2625 [hep-ph].
 - [12] I. Bediaga, T. Frederico, and O. Lourenço, *Phys. Rev. D* **89**, 094013 (2014), arXiv:1307.8164 [hep-ph].
 - [13] J. H. Alvarenga Nogueira, I. Bediaga, A. B. R. Cavalcante, T. Frederico, and O. Lourenço, *Phys. Rev. D* **92**, 054010 (2015), arXiv:1506.08332 [hep-ph].
 - [14] R. Álvarez Garrote, J. Cuervo, P. C. Magalhães, and J. R. Peláez, *Phys. Rev. Lett.* **130**, 201901 (2023), arXiv:2210.08354 [hep-ph].
 - [15] T. Mannel, K. Olschewsky, and K. K. Vos, *JHEP* **06**, 073 (2020), arXiv:2003.12053 [hep-ph].
 - [16] U.-G. Meißner and S. Gardner, *Eur. Phys. J. A* **18**, 543 (2003).
 - [17] B. Ananthanarayan, G. Colangelo, J. Gasser, and H. Leutwyler, *Phys. Rept.* **353**, 207 (2001), arXiv:hep-ph/0005297.

- [18] G. Colangelo, J. Gasser, and H. Leutwyler, *Nucl. Phys. B* **603**, 125 (2001), [arXiv:hep-ph/0103088](#).
- [19] R. García-Martín, R. Kamiński, J. R. Peláez, J. Ruiz de Elvira, and F. J. Ynduráin, *Phys. Rev. D* **83**, 074004 (2011), [arXiv:1102.2183 \[hep-ph\]](#).
- [20] I. Caprini, G. Colangelo, and H. Leutwyler, *Eur. Phys. J. C* **72**, 1860 (2012), [arXiv:1111.7160 \[hep-ph\]](#).
- [21] J. R. Peláez, P. Rabán, and J. Ruiz de Elvira, *Phys. Rev. D* **111**, 074003 (2025), [arXiv:2412.15327 \[hep-ph\]](#).
- [22] U.-G. Meissner and J. A. Oller, *Nucl. Phys. A* **679**, 671 (2001), [arXiv:hep-ph/0005253](#).
- [23] R. Omnès, *Nuovo Cim.* **8**, 316 (1958).
- [24] K. M. Watson, *Phys. Rev.* **95**, 228 (1954).
- [25] L. Wolfenstein, *Phys. Rev. D* **43**, 151 (1991).
- [26] M. Suzuki and L. Wolfenstein, *Phys. Rev. D* **60**, 074019 (1999), [arXiv:hep-ph/9903477](#).
- [27] H.-Y. Cheng, C.-K. Chua, and Z.-Q. Zhang, *Phys. Rev. D* **94**, 094015 (2016), [arXiv:1607.08313 \[hep-ph\]](#).
- [28] J. T. Daub, C. Hanhart, and B. Kubis, *JHEP* **02**, 009 (2016), [arXiv:1508.06841 \[hep-ph\]](#).
- [29] B. Kubis and J. Plenzer, *Eur. Phys. J. C* **75**, 283 (2015), [arXiv:1504.02588 \[hep-ph\]](#).
- [30] P. Büttiker, S. Descotes-Genon, and B. Moussallam, *Eur. Phys. J. C* **33**, 409 (2004), [arXiv:hep-ph/0310283](#).
- [31] J. R. Peláez and A. Rodas, *Eur. Phys. J. C* **78**, 897 (2018), [arXiv:1807.04543 \[hep-ph\]](#).
- [32] J. R. Peláez and A. Rodas, *Phys. Rept.* **969**, 1 (2022), [arXiv:2010.11222 \[hep-ph\]](#).
- [33] A. Pich, E. Solomonidi, and L. Vale Silva, *Phys. Rev. D* **108**, 036026 (2023), [arXiv:2305.11951 \[hep-ph\]](#).
- [34] J. F. Donoghue, J. Gasser, and H. Leutwyler, *Nucl. Phys. B* **343**, 341 (1990).
- [35] B. Moussallam, *Eur. Phys. J. C* **14**, 111 (2000), [arXiv:hep-ph/9909292](#).
- [36] S. Descotes-Genon, *JHEP* **03**, 002 (2001), [arXiv:hep-ph/0012221](#).
- [37] M. Hoferichter, C. Ditsche, B. Kubis, and U.-G. Meißner, *JHEP* **06**, 063 (2012), [arXiv:1204.6251 \[hep-ph\]](#).
- [38] J. T. Daub, H. K. Dreiner, C. Hanhart, B. Kubis, and U.-G. Meißner, *JHEP* **01**, 179 (2013), [arXiv:1212.4408 \[hep-ph\]](#).
- [39] A. Celis, V. Cirigliano, and E. Passemar, *Phys. Rev. D* **89**, 013008 (2014), [arXiv:1309.3564 \[hep-ph\]](#).
- [40] M. W. Winkler, *Phys. Rev. D* **99**, 015018 (2019), [arXiv:1809.01876 \[hep-ph\]](#).
- [41] S. Ropertz, C. Hanhart, and B. Kubis, *Eur. Phys. J. C* **78**, 1000 (2018), [arXiv:1809.06867 \[hep-ph\]](#).
- [42] L.-L. Chau and W.-Y. Keung, *Phys. Rev. Lett.* **53**, 1802 (1984).
- [43] L. Wolfenstein, *Phys. Rev. Lett.* **51**, 1945 (1983).
- [44] I. Bediaga, T. Frederico, and P. C. Magalhães, *Phys. Lett. B* **806**, 135490 (2020), [arXiv:2003.10019 \[hep-ph\]](#).
- [45] N. N. Khuri and S. B. Treiman, *Phys. Rev.* **119**, 1115 (1960).
- [46] F. Niecknig and B. Kubis, *Phys. Lett. B* **780**, 471 (2018), [arXiv:1708.00446 \[hep-ph\]](#).
- [47] D. Stamen, T. Isken, B. Kubis, M. Mikhasenko, and M. Niehus, *Eur. Phys. J. C* **83**, 510 (2023), [Erratum: *Eur. Phys. J. C* **83**, 586 (2023)], [arXiv:2212.11767 \[hep-ph\]](#).
- [48] E. Kou, T. Moskalets, and B. Moussallam, *JHEP* **12**, 177 (2023), [arXiv:2303.12015 \[hep-ph\]](#).
- [49] S. Holz, C. Hanhart, M. Hoferichter, and B. Kubis, *Eur. Phys. J. C* **82**, 434 (2022), [Addendum: *Eur. Phys. J. C* **82**, 1159 (2022)], [arXiv:2202.05846 \[hep-ph\]](#).
- [50] G. Colangelo, M. Hoferichter, B. Kubis, and P. Stoffer, *JHEP* **10**, 032 (2022), [arXiv:2208.08993 \[hep-ph\]](#).
- [51] J. M. Dias, T. Ji, X.-K. Dong, F.-K. Guo, C. Hanhart, U.-G. Meißner, Y. Zhang, and Z.-H. Zhang, *Phys. Rev. D* **111**, 014031 (2025), [arXiv:2409.13245 \[hep-ph\]](#).
- [52] A. Furman, R. Kamiński, L. Leśniak, and B. Loiseau, *Phys. Lett. B* **622**, 207 (2005), [arXiv:hep-ph/0504116](#).
- [53] B. El-Bennich, A. Furman, R. Kamiński, L. Leśniak, and B. Loiseau, *Phys. Rev. D* **74**, 114009 (2006), [arXiv:hep-ph/0608205](#).
- [54] B. El-Bennich, A. Furman, R. Kamiński, L. Leśniak, B. Loiseau, and B. Moussallam, *Phys. Rev. D* **79**, 094005 (2009), [Erratum: *Phys. Rev. D* **83**, 039903 (2011)], [arXiv:0902.3645 \[hep-ph\]](#).
- [55] D. Boito, J. P. Dedonder, B. El-Bennich, R. Escribano, R. Kamiński, L. Leśniak, and B. Loiseau, *Phys. Rev. D* **96**, 113003 (2017), [arXiv:1709.09739 \[hep-ph\]](#).
- [56] W. H. Press, S. A. Teukolsky, W. T. Vetterling, and B. P. Flannery, *Numerical Recipes 3rd Edition: The Art of Scientific Computing*, 3rd ed. (Cambridge University Press, USA, 2007).